CALIBRATION TRIALS OF WORKING CAPABILITIES OF THE NEW HYPERSONIC WIND TUNNEL AT-303 AT ITAM

A.M. Kharitonov, V.I. Zvegintsev, N.P Adamov, L.G. Vasenev, A.D. Kuraeva, D.G. Nalivajchenko, A.V. Novikov, S.I. Shpak, V.F. Chirkashenko

Institute of Theoretical and Applied Mechanics, Russian Academy of Sciences, Siberian Branch, Novosibirsk, Russia

1. Wind tunnel AT-303 description

The new hypersonic wind tunnel AT-303 is now in operation at the Institute of Theoretical and Applied Mechanics [1, 2]. A total view and sketch of this hypersonic adiabatic compression wind tunnel AT-303 is presented in Fig. 1. The basis of the wind tunnel consists in a test gas source, which is the most complex and innovative part of the wind tunnel. Two main pistons are moving in the high-pressure section of the gas source, thus adiabatically compressing the test gas within the settling chamber up to a pressure of 3000 bar with a temperature of 2500 K. After compression a fast-acting valve (nozzle shutter) in the settling chamber is opened, and an air flow through the nozzle is formed. The pistons keep moving during flowing out then the pistons stop and the run is over.

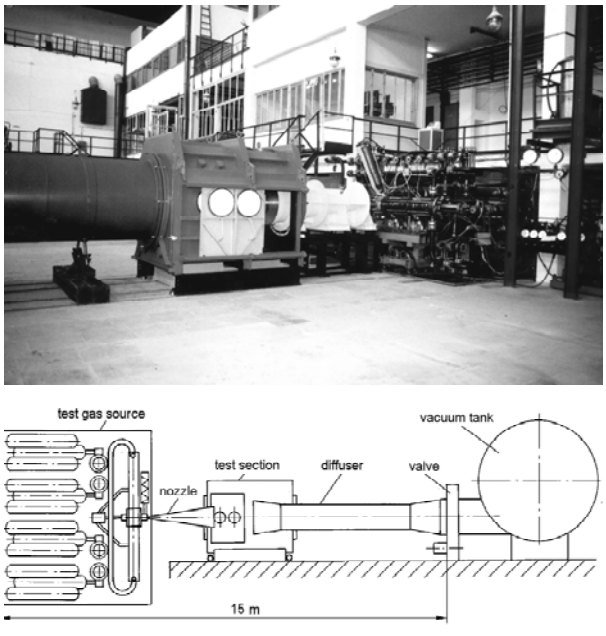

Fig. 1

The remaining elements of the wind tunnel are typical for hypersonic wind tunnels: a conical nozzle with a total angle of 16°, a test section, an exhaust diffuser, a large-scale vacuum valve, and a vacuum tank outside. AT-303 with an initial electric heater provides from 1 to 3.6 dm^3 of pressurized air, which is sufficient for a run duration from 40 to 200 ms with the conical nozzle exit diameter of 300 and 600 mm in the flow Mach number range between M = 8 and M = 20. In addition high

purity of the test gas, long run duration, and relatively large-scale nozzle are provided by the facility, which is sufficient for on-ground testing of promised hypersonic vehicles.

2. Measurement techniques

The new wind tunnel operates automatically under computer guidance. As a whole, the control system contains 65 digital and analog I/O channels. The control system allows automatic preparation of the wind tunnel to the experiment with prescribed initial parameters. The measurement system consists of two subsystems: high-accuracy subsystem and normal-accuracy subsystem. The high-accuracy subsystem is based on the SCP-3200 multichannel measurement and data acquisition system produced by Eckelmann Steuerungstechnik GmbH. Each channel of this measurement system contains a high-accuracy amplifier, low-frequency filter with a controlled sampling frequency, analog-to-digital converter (up to 1 million samples per second), and digital memory (up to 512,000 samples). All the channels used are turned on and operate simultaneously. Currently, the high-accuracy subsystem has 52 measurement channels. The test results are collected to unified database, which store all the necessary information about the wind-tunnel parameters, particular, model, and test conditions.

The optical system includes two optical devices: the shadow pictures device IAB-451 with a 230-mm diameter of the vision field, which is well known in Russia, and a unique holographic interferometer IZK-462 with a 400-mm vision field. Both these devices are hung up on united lavaliere, which can easily move along the windows of the test section. For picture registration, there is a unique high-speed CCD camera up to 2500 frames per second and with a memory volume of 512 Mbytes for data accumulation. All measurement techniques used are based on long-time experience of short-duration facilities exploitation at the Institute of Theoretical and Applied Mechanics.

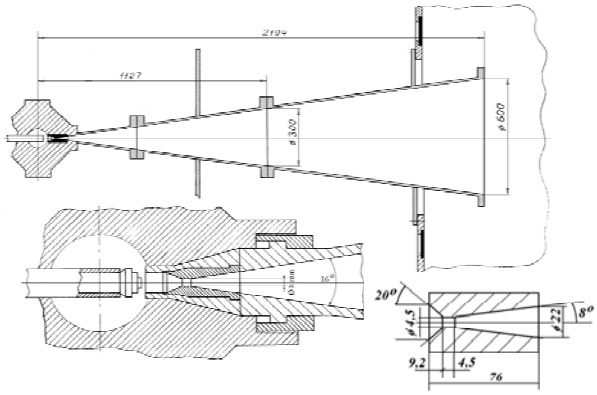

Fig. 2

A conical nozzle with angle of 16^0 was chosen as the first step during AT-303 development. The design of conical nozzle is very simple and its fabrication is not so expensive. What is more attractive a flow Mach number at the nozzle exit is easy adjusted in a wide range by small throat insert replacement. A sketch of the nozzle is shown in Fig. 2.

3. Mach number measurements at the nozzle exit

A combined rake of total-pressure P_0' and heat-flux probes involved for the velocity field at the nozzle exit and downstream from the nozzle measurements. The combined rake consists of two plate-type rakes with a set of heat-flux probes and total-pressure probes, which are orthogonally fixed on a sting. The diameter of the probes used for total pressure measurement is 2 mm. In the experiments, the sting of the rake was mounted in the test section and could be axially rotated in the range from 0 to 360° with a step of φ = 45°. The measurements were performed in the following sequence. For a given operation mode of the wind tunnel, for which the flow quality was examined, 3 to 5 cross sections spaced by 100–150 mm in the working zone were chosen. After that, the wind tunnel was started, and the readings of all probes of the rake were registered. The measurements were mainly performed with two mutually perpendicular positions of the rake:

$\varphi = 0$ and $\varphi = 90°$. In some regimes, additional measurements were performed for the rake angle $\varphi = \pm 45°$. In some experiments, the flow around the measurement rake was visualized, which allowed monitoring of the boundary-layer boundaries and origination of oblique shocks at the exit in the off-design regimes of nozzle operation.

In addition to pressure $P_0^{'}$ measurements the total pressure in the settling chamber of the wind tunnel was measured in each experiment, and the stagnation temperature was calculated. The initial data for calculations were gas pressure measurements in the settling chamber. From this record the initial pressure $P_0(0)$ and initial temperature $T_0(0)$ reached after the settling chamber is filled. The initial temperature $T_0(0)$ of the test gas is determined from the measured temperature of the heater with the use of a previously obtained dependence between the heater temperature and gas temperature after filling the chamber. The further change in gas temperature $T_0(t)$ in the course of compression and exhaustion from the settling chamber was calculated by the measured values of pressure $P_0(t)$ with the use of adiabatic formulas for real high-density air. Mach numbers $M_j(t)$ for each j-point of the flow were determined from the ratios $P_{j0}'(t)/P_0(t)$ in a real air isentropic expansion process.

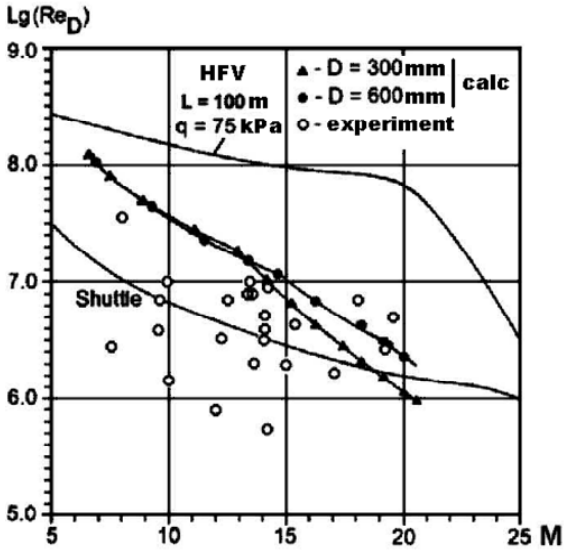

Fig. 3

Based on the calculated Mach numbers, the flow core with deviations from the general mean value less than 5% was determined; then, the mean Mach number for a particular cross section was found from the data of probes inside the flow core. When Mach number is known the main flow parameters were determined as a calculation results for isentropic expansion of the gas, namely: static pressure of the flow $P(t)$, static temperature $T(t)$, velocity $V(t)$, dynamic pressure $q(t)$, and Reynolds number per meter $\mathrm{Re}_1(t)$.

The total estimate of the error in measuring the Mach number does not exceed $\varepsilon(\mathrm{M}) = 1.4\%$.

27 operation regimes were examined in the range of Mach numbers from M = 8 to M = 20 in accordance with the technology described above. These test regimes are plotted by the open discs in coordinates of the Mach and Reynolds numbers (see Fig. 3). The upper curve corresponds to the typical trajectory of a promising scramjet-powered hypersonic vehicle (L = 100 m) at a dynamic pressure q = 75 kPa. The lower curve corresponds to the Space Shuttle or Buran ($L \approx 45$ m) re-entry trajectory. As is seen from this figure, the wind tunnel AT-303 ensures full simulation of real Mach and Reynolds numbers not only for small-scale hypersonic objects but also for large-scale vehicles, as well as for advanced scramjet-powered atmospheric spaceplanes.

4. Uniformity of the velocity field in the test section of AT-303.

Typical experimental results of flowfield measurements are presented in Fig. 4. The mean values of Mach number in the flow core comprise M = 18 for this example.

The root-mean-square deviations in the flow core, which characterize the degree of non-uniformity or the flow quality, are shown in Fig. 5 versus the Mach number. As a whole, it is seen that estimate of non-uniformity in the flow

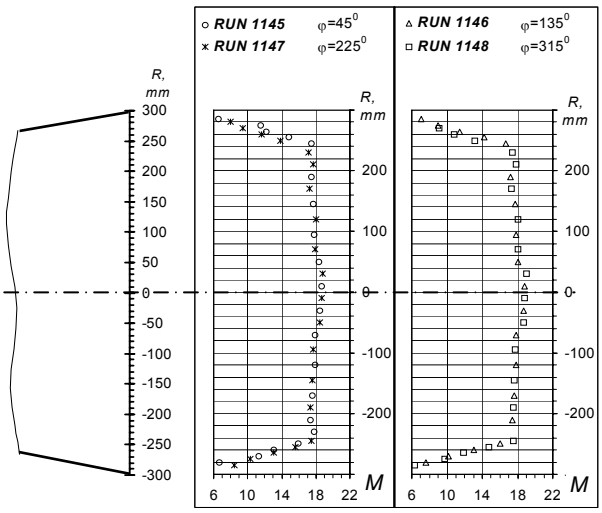

Fig. 4. D_n = 600 mm, d^* = 6.5 mm, P_0 = 153.08 MPa, T_0 = 1587 K, M_{mean} = 18, σ_M = 2.74%, q = 18.1 kPa, $Re_1 = 1.18 \cdot 10^7$

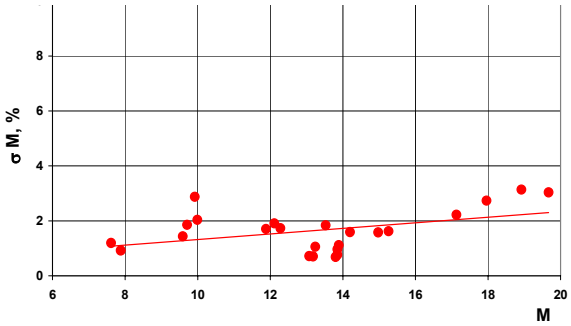

Fig. 5. Non-uniformity of the velocity field at the exit of the conical nozzle of the wind tunnel AT-303

core from the conical nozzle of the AT-303 wind tunnel varies from 1% to 3%, slightly increasing with increasing Mach number.

The mean values of the Mach number increase downstream (see Fig. 6), which is typical of the conical nozzle. In the zone where the models are located $0 \le X \le 300$ mm, the Mach number increases by 10% and 5% for the nozzles with the exit diameters 300 and 600 mm, respectively. It is of interest to note that the change in the Mach number obtained experimentally is in good agreement with the expected values for the conical flow of a perfect gas ($\gamma = 1.4$) downstream of the nozzle to the chosen cross section. A simple calculation offers a rather good prediction of the increase in

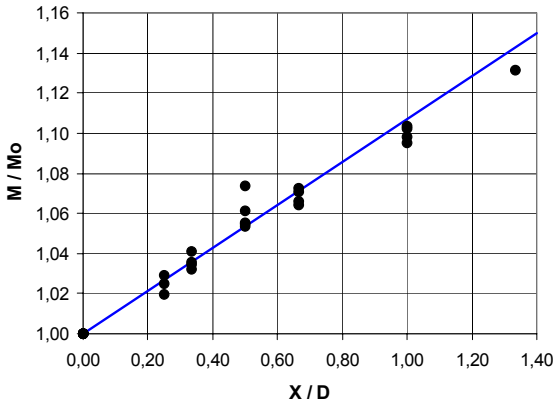

Fig. 6. Increment in the Mach number downstream of the nozzle exit

the Mach number because the flow in this region is rather close to the ideal gas flow.

The observed deviations from the mean values do not exceed current requirements to uniformity of the fields of flow parameters in hypersonic short-duration wind tunnels. It should be noted that these estimates of uniformity of velocity fields include both the instrumental errors of measurement and the errors of reproducibility of test conditions in individual runs.

As an example, the Mach number fields at the exit of the conical nozzle of the AT-303 wind tunnel and at the exit of the contoured

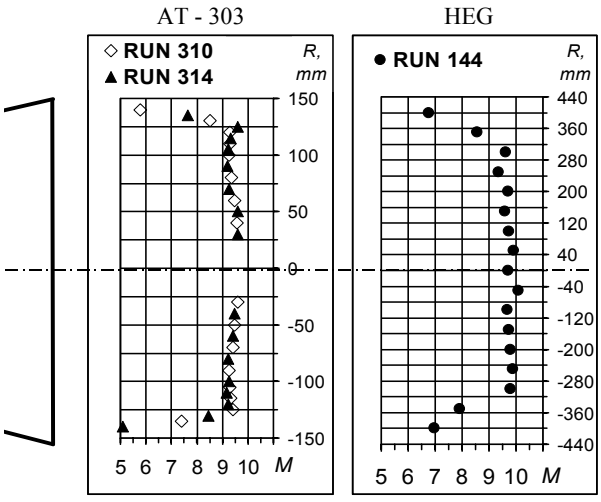

Fig. 7. Comparison of Mach number distributions at the nozzle exit for AT-303 and HEG. M_{mean}=9.5; P_0 = 29.4 MPa; M_{mean} = 9.7; P_0 = 111 MPa; σ_{Mmean} = 1.5%; T_0 = 1000 K; σ_{Mmean} = 1.8%; T_0 = 8113 K

nozzle of the high-enthalpy wind tunnel HEG (DLR) [3] are compared in Fig. 7. It is seen that the non-uniformity of Mach number fields in both wind tunnels is approximately identical and reaches 1.5–1.8%.

5. Heat fluxes measurement at the nozzle exit

The non-uniformity of heat-flux distribution in the test section of AT-303 was determined with the use of thermocouple-type calorimetric probes. The design of this probe was developed and manufactured at ITAM (see Fig. 8).

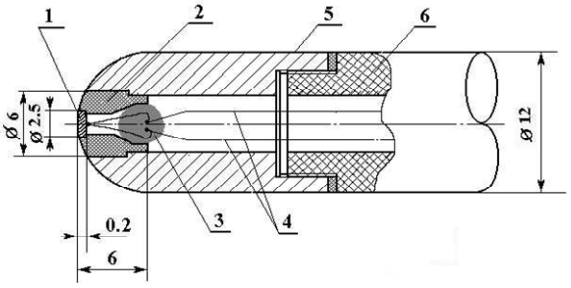

Fig. 8. Layout of the heat-flux probe. 1 – calorimeter; 2 – heat insulator; 3 – glue; 4 – thermocouple wires; 5 – probe body; 6 – insulating insert

The main element of the probe is the calorimeter (1) made in the form of a copper disk 2.5 mm in diameter and 0.2 mm thick; the disk was connected through a thermal insulator (2) in the vicinity of the stagnation point of the hemisphere of the probe body (5) as a spherically blunted cylinder 12 mm in diameter.

The theory of calorimetric method of heat flux measurement was described in detail in [4, 5]. The value of the heat flux is determined under the thin-wall assumption with regular heat transfer in the course of unsteady heating of the calorimeter. The temperature gradients in time on the frontal and rear surfaces of the calorimeter become identical, and the specific heat flux is determined as $\dot{q} = \frac{1}{A} \cdot \frac{dQ}{dt} = \frac{m \cdot c}{A} \cdot \frac{dT}{d\tau}$ where m is the calorimeter mass, A is the frontal surface area of the calorimeter, C_P is the specific heat, and $\frac{dT}{d\tau}$ is the gradient of the mean temperature of the calorimeter.

In experiments the heat flux was determined from the measured results by the following equation: $\dot{q}_i = \left(dU/d\tau\right)_i \cdot K_i \frac{MW}{m^2}$. where K_i – the conversion coefficients of the probe, which establish the relation between the heat flux and temperature gradient in time.

The conversion coefficients of the self-made probes, were determined by means of individual dynamic calibration of each probe under conditions of convective heat transfer on the jet pulse thermal calibration device in TsAGI [6].

In all experiments, the signals were registered during run by 12-bit ADC with a time resolution of 0.1 ms. The filtration system eliminated network noise pickup on the measured signal.

The total error of determining the heat flux, including the random and systematic errors, is within 10%. It is caused by deviations of geometric dimensions from the design values, heat transfer to thermocouple wires, temperature averaging on the calorimeter surface, heating of cold junctions of thermocouples, and algorithms for signal processing.

6. Discussion of heat-flux measurement results

Typical results on the thermal non-uniformity of the flow in the transverse direction can be drawn from the Fig. 9. In Fig. 10 relative thermal non-uniformity of the flow in the cross section versus the Mach number at the nozzle exit is exhibited. It is seen that for M < 15, the heat-flux non-uniformity varies from 1.5% to 10%. The change in the level of the thermal non-uniformity with distance from the nozzle is not ordered. A possible reason is the error of the heat-flux probes used (~10%), which corresponds to the range of scatter of thermal non-uniformity over the cross sections.

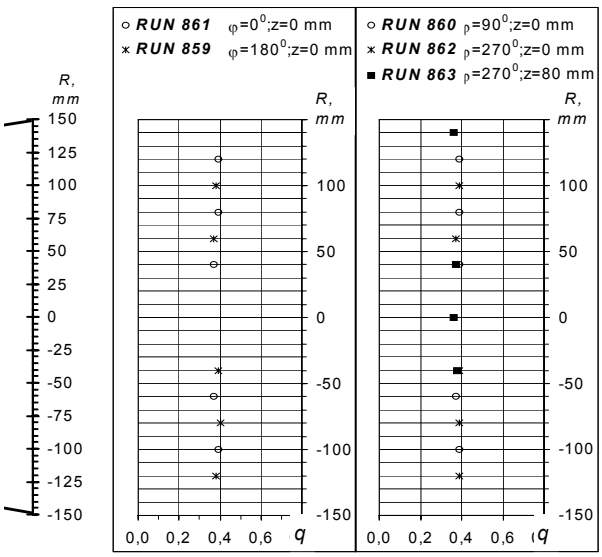

Fig. 9. Typical distribution of heat-fluxes D_n = 300 mm, d^* = 14 mm, X = 300 mm, q_{mean} = 0.382 MW/m^2, σ_{mean} = 2.96%, P_0 = 18.34 MPa, T_0 = 1063 K, M = 10.6, Re_1=1.06·10^7

For M > 15, the thermal non-uniformity of the flow increases up to 15%. This trend to increasing is in line with the increase in non-uniformity of the flow in terms of the Mach number. The sizes of uniform thermal core coincide with flow core determined by the Mach number measurements.

The levels of the longitudinal thermal non-uniformity at distances $\overline{X} \le 0.5$ from the nozzle are commensurable with the transverse thermal non-uniformity. In the cross section $\overline{X} = 1.0$, the heat-flux level decreases by 30%,

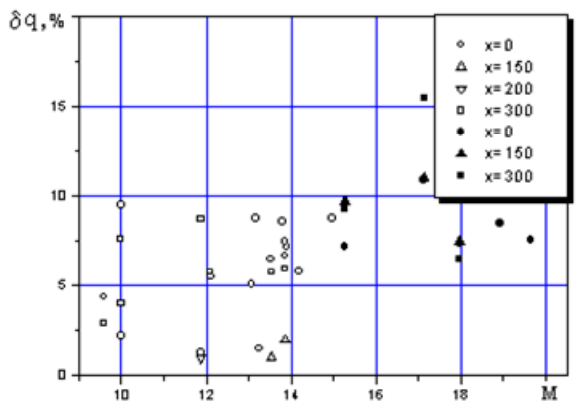

Fig. 10. Transverse thermal non-uniformity of the flow in AT-303

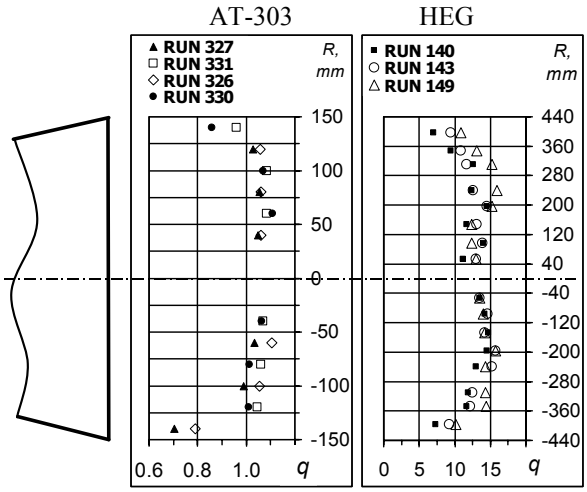

Fig. 11. Comparison of heat fluxes distribution in AT-303 and high-enthalpy wind tunnel HEG. M = 9.4; P_0 = 29.4 MPa, M = 10; P_0 = 111 MPa, T_0 = 1000 K; σ_q = 2.9%, T_0 = 8113 K; σ_q = 9.3%

as compared to the corresponding value at the nozzle exit.

The heat-flux fields at the exit of the conical nozzle of the AT-303 wind tunnel and the contoured nozzle of the high-enthalpy wind tunnel HEG (DLR) [3] are compared in Fig. 11. The non-uniformity of the heat-flux field in HEG is approximately three times higher than the non-uniformity of heat fluxes in AT-303, which seems to be related to a significantly higher level of temperatures in HEG.

7. HB-2 model description

The necessity of having a certain reference model for comparison of experimental data obtained in different wind tunnels gave impetus to the development of a number of models of different geometric configurations (the so-called series of AGARD reference models). In particular, for high-velocity wind tunnels, the Supersonic Tunnels Association (STAI) adopted two new geometric configurations of a hypersonic ballistic model, which were cylinders with a blunted cone forebody and with or without the expanding rear part. These configurations were denoted as HB-2 and HB-1 models and, on the basis of review

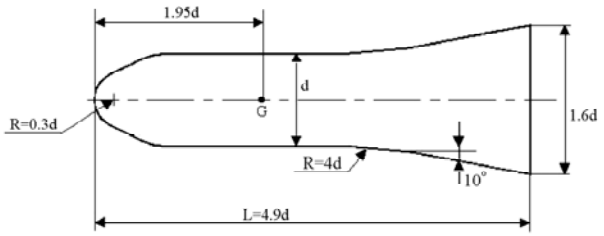

Fig. 12. The contour of HB-2 model and its relative sizes

of their aerodynamic characteristics measured in different wind tunnels of the US, France, and Germany, were included into the series of AGARD reference models [7]. Therefore, to validate the quality of the measurement and computational systems of the AT-303 wind tunnel, the aerodynamic characteristics of reference model were measured in this new hypersonic facility. The HB-2 configuration ($d = 60$ mm) was chosen as the basic model (see Fig. 12). The model is made of an aluminum alloy; its weight is equal to 0.97 kg. The aerodynamic loads and moments acting on the HB-2 reference model were measured by an internal six-component strain-gauge balance designed and manufactured at TsNIIMASh. Test conditions are collected in the table.

Table

D nozzle, mm	300				600	600
Mach	10		12		12	15,6
Re_d*10^6	1,39	0,35	0,68	0,26	0,13	0,37
AOA, deg	-4 – +12					

To estimate the magnitude of the random error of measurement of aerodynamic coefficients of the HB-2 model, a series of seven tests without taking the model off the wind-tunnel suspending devices was performed under the following conditions: M = 9.7; $\alpha = 10°$; $Re_d = 1.39\ 10^6$. Statistical processing of results allowed us to calculate the root-mean-square deviations for the drag force coefficient- $\sigma_{C_A} = 0.005$, for the normal force coefficient – $\sigma_{C_Z} = 0.006$, for the pitching moment coefficient – $\sigma_{C_m} = 0.001$.

8. Comparison of aerodynamic characteristics of the HB-2 model obtained in different wind tunnels.

The basis for comparison of aerodynamic characteristics of the HB-2 model was formed by the aerodynamic characteristics of the coefficients C_A, C_Z, and C_m as functions of the angle of attack, which were published [7] in the graphical form. Here the aerodynamic characteristics of the model are exhibited that were measured at $M = 10$ in the wind tunnel C of the von Karman Gas-Dynamics Facilities of the Arnold Engineering Development Center (VKF, AEDC, USA) and in the wind tunnel R3 of the Laboratory of Aerodynamics and Material Science (ONERA, France); as well as the data obtained at M = 16.5 in the wind tunnel ARC1 of the Laboratory of Aerodynamics of ONERA.

In the Fig. 13 drag coefficient of the model at $M = 10$ is presented. The open symbols □ and ◊ show the aerodynamic coefficients measured in AT-303 and processed by the method with filtration and averaging, and the filled symbols indicate the same results that contain a correction, which follows from calculations of the model aerodynamic characteristics produced by uniform or conical flow. I.I. Mazul performed these calculations. It is seen the correction for conicity yields good

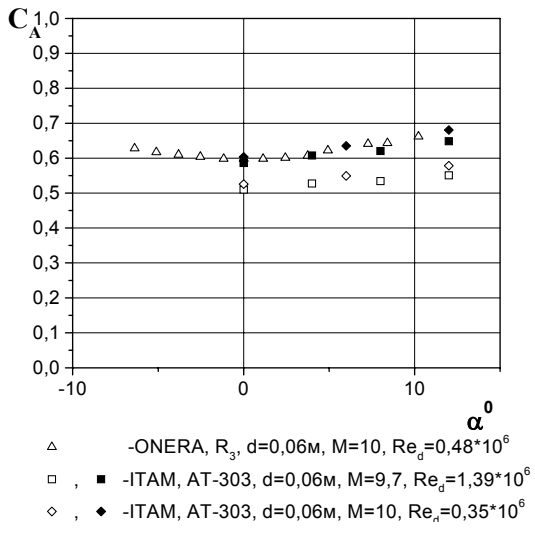

Fig. 13. The drag force coefficients for HB-2

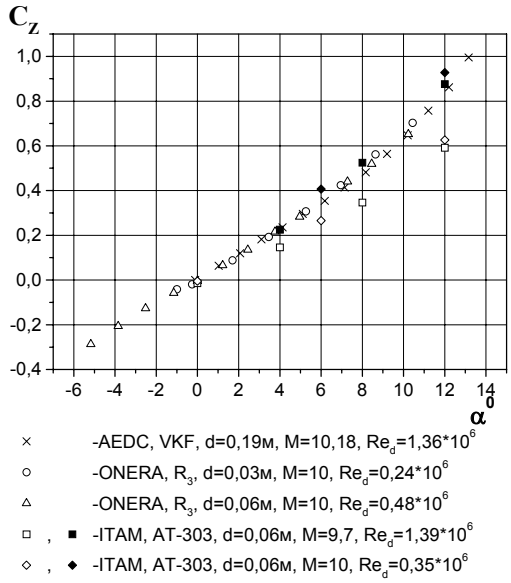

Fig. 14

agreement of the coefficients C_A of models of identical size for similar test conditions in terms of the Reynolds number.

The normal force coefficients C_Z are compared in Fig. 14. As a whole the data obtained for $M = 10$ in the wind tunnel C, VKF and AT-303 for $Re_d = 1.39\ 10^6$ and with allowance for flow conicity are in good agreement. The difference in the coefficients C_Z measured in AT-303 for $Re_d = 0.35\ 10^6$ and in R3, ONERA, for $Re_d = 0.48\ 10^6$, is less then 9÷10%.

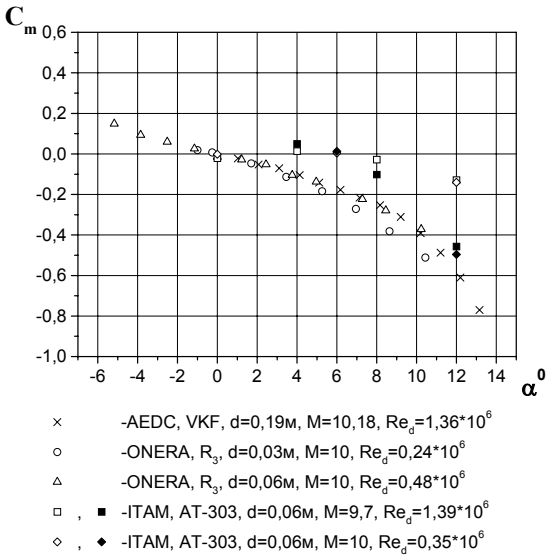

Fig. 15

Fig. 15 shows the dependence $C_m = f(\alpha)$. In this case flow conicity correction based on calculations did not bring a good correlation in a pitching moment especially at α from 4 to 10 deg. The noticeable difference in the coefficients C_m obtained in the wind AT-303 is caused, in the author's opinion, by limitation of used technique of calculations. We can assume that good agreement can be achieved by measuring moments with contoured nozzles.

9. Acknowledgments

The work was performed during a few years by a large team of researchers at ITAM and became possible due to support of collaborators of the ISTC project No 2109, Gerard Laruelle and Jean-Claude Paulat (EADS, Space Transportation, Research Directorate), Dr. Wilhelm Kordulla and J-M. Muylaert (ESA ESTEC). This support is gratefully acknowledged.

10. Conclusion

At the Institute of Theoretical and Applied Mechanics of the Siberian Branch of the Russian Academy of Sciences the new hypersonic AT-303 wind tunnel has been created, which ensures unique possibilities for investigating aerothermodynamic problems related to promising hypersonic vehicles with air-breathing engines.

During years, more than 1400 runs of the new wind tunnel were performed and several experimental programs were fulfilled. The characteristics of the generated flow were primarily examined within the entire range of test regimes. The non-uniformity of the velocity field at the exit of the conical nozzle used in this facility is less than 3% within the Mach number range from 8 to 20. Non-uniformity of the heat fluxes distribution in the cross section of the flow amounts up to 10%.

The flow quality and performance of instrumentation of the AT-303 wind tunnel are checked by testing of the HB-2 reference model with force measurements. Comparison of aero-

dynamic characteristics obtained with available experimental data from wind tunnels of Germany, France, and USA show that the AT-303 wind tunnel and its measurement system allow obtaining reliable and credible results.

11. References

[1] Kharitonov A.M., Shyshov V.I., Vyshenkov Ju.I., Topchian M.E., Zvegintsev V.I., Rychkov V.N., Mescherjakov A.A., Pinakov V.I. Simulation of hypersonic scramjet-powered flying vehicles in adiabatic compression facilities with pressure multipliers. Proc. of the 3rd European Symposium on Aperothermodynamics for Space Vehicles, ESTEC, Noordwijk, The Netherlands, Nov. 24 – 26, 1998. ESA SP-426.

[2] Kharitonov A.M., Zvegintsev V.I., Fomin V.M., Topchyan M.E., Mescherjakov A.A., Pinakov V.I., New-Generation Hypersonic Adiabatic Compression Facilities with Pressure Multiplier. *Advanced Hypersonic Test Facilities*, edited by Frank Lu and Dan Marren, Progress in Astronautics and Aeronautics, v.198, Chapter 22, 2002, pp.585-619.

[3] Beck W.H., Eitelberg G., Mcintyre T.J. The high enthalpy shock tunnel in Gottingen HEG. 3rd Aerospace symposium, Aug.1991, Braunschweig, pp. 53-63.

[4] Erhart W., Bainum D. Measurement equipment of a hypersonic hotshot wind tunnels. In: Techniques of Hypersonic Investigations. Moscow, 1964, pp. 320-350.

[5] Ledford R.L. Probe for measuring specific heat flux in hypersonic wind tunnels. In: Advanced Techniques of Aerodynamic Investigations at Hypersonic Velocities, Mashinostroenie, Moscow, 1965, pp. 458-469.

[6] Bogdanov V.V., Kalachinskii Yu.Yu., Pleshakova L.A. Instrumentation for measuring heat-flux density in short-duration wind tunnels. Trudy TsAGI, No. 1978, 1979, pp. 27-34. (In Russian).

[7] Ceresuela R. Maquettes Etalons HB-1 et HB-2. Caracteristiques aerodynamiques mtsurees dans les souffleries de l'O.N.E.R.A. de Mach 2 a Mach 16,5, Note Technique № 123, 1968.